

Regular Articles

Temperature insensitive curvature sensor based on cascading photonic crystal fiber

Guangwei Fu*, Yunpu Li, Xinghu Fu, Wa Jin, Weihong Bi*

School of Information Science and Engineering, The Key Laboratory for Special Fiber and Fiber Sensor of Hebei Province, Yanshan University, Qinhuangdao, Hebei 066004, China

ARTICLE INFO

Keywords:

Fiber optics
Cascading
Photonic crystal fiber
Temperature insensitive
Curvature

ABSTRACT

A temperature insensitive curvature sensor is proposed based on cascading photonic crystal fiber. Using the arc fusion splicing method, this sensor is fabricated by cascading together a single-mode fiber (SMF), a three layers air holes structure of photonic crystal fiber (3PCF), a five layers air holes structure of photonic crystal fiber (5PCF) and a SMF in turn. So the structure SMF-3PCF-5PCF-SMF can be obtained with a total length of 20 mm. During the process of fabrication, the splicing machine parameters and the length of each optical fiber are adjusted to obtain a high sensitivity curvature sensor. The experimental results show that the curvature sensitivity is -8.40 nm/m^{-1} in the curvature variation range of $0-1.09 \text{ m}^{-1}$, which also show good linearity. In the range of $30-90 \text{ }^\circ\text{C}$, the temperature sensitivity is only about $3.24 \text{ pm}/^\circ\text{C}$, indicating that the sensor is not sensitive to temperature. The sensor not only has the advantages of easy fabricating, simple structure, high sensitivity but also can solve the problem of temperature measurement cross sensitivity, so it can be used for different areas including aerospace, large-scale bridge, architectural structure health monitoring and so on.

1. Introduction

The relative displacement and deformation measurement play an important role in aerospace, geophysics, large bridges, building structure, health detection and other fields. And bending curvature measurement is one of the important parameters to measure the displacement and deformation. Traditional measurement methods for curvature commonly use electrical method, but it has some disadvantages such as slow response speed, low sensitivity, susceptible to electromagnetic interference and so on. In recent years, fiber optic sensors have the obvious advantages of small size, fast response speed, high sensitivity, anti-electromagnetic interference, permissible embedment and so on, which have caused great interests among many researchers all over the world. Much research about curvature optical fiber sensor have been reported, such as fiber Bragg grating (FBG) [1–3], long period fiber grating (LPFG) [4–6], multicore fiber [7–9], Mach-Zehnder (M-Z) structure [10], core-offset structure [11], and the conical structure of photonic crystal fibers [12], etc. Compared with other optical fiber curvature sensors based on PCF, this presenting cascaded structure may improve the curvature sensitivity in experiment. For example, the curvature sensitivity of tapered PCF sensor is $-5.39297 \text{ nm/m}^{-1}$ [13], and the curvature sensitivity of bend sensor based on Mach-Zehnder interferometer using photonic crystal fiber is 3.046 nm/m^{-1} [14].

These different kinds of optical fiber curvature sensors greatly promote the development of the curvature measuring devices, laying a solid foundation on the progress of different structure curvature optical fiber sensor.

A temperature insensitive curvature sensor is proposed based on cascading photonic crystal fiber (PCF). The sensor is fabricated by cascading together a single-mode fiber (SMF), a three layers air holes structure of photonic crystal fiber (3PCF), a five layers air holes structure of photonic crystal fiber (5PCF) and a SMF in turn. In this paper, the cascading structure of curvature optical fiber sensor for sensing experiment is studied, and the relationship between different curvature and wavelength drift is researched. In addition, analysis has been done on the temperature sensing properties of the sensor.

2. Basic principle

The structure of temperature insensitive curvature sensor based on cascading photonic crystal fiber is shown in Fig. 1. It is made by cascading structure with SMF, 3PCF, 5PCF, SMF in turns.

As shown in Fig. 1, after the transmission light from input end of SMF passing the first fusion splicing joint, a part of light is coupled into 3PCF core and the rest enters into the cladding layer, transmitted by fiber core mode and cladding mode at first collapsing areas (CA1),

* Corresponding authors.

E-mail addresses: earl@ysu.edu.cn (G. Fu), whbi@ysu.edu.cn (W. Bi).

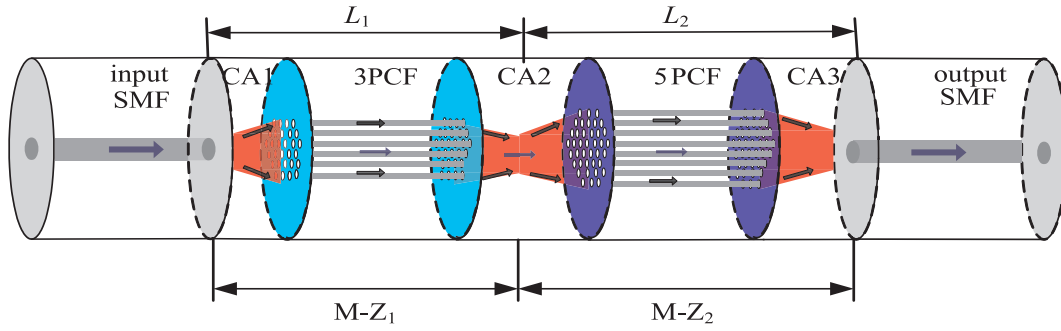


Fig. 1. The structure of SMF-3PCF-5PCF-SMF.

respectively. When the transmission light goes through the second fusion splicing joint, fiber core mode and cladding mode of 5PCF are inspired because of air holes collapse at second collapsing areas (CA2). In the end, they are coupled into the output end of SMF and be transmitted to the third fusion splicing joint, which is at the third collapsing areas (CA3). Due to the difference of propagation constant between fiber core mode and cladding mode, there is phase difference after transmitting a certain distance, thus it will cause interference in the related fusion splicing joints and form Mach-Zehnder structure, briefly, the transmission light goes through 3PCF and forms M-Z₁ structure. When the transmission light goes through 5PCF, it will form M-Z₂ structure. Because there is always a cladding mode of energy distribution which plays a leading role among numerous cladding modes, it can be simplified by double beam interference theory. Thus transmission light after M-Z₁ will have a certain phase change, which can be used as the initial phase of M-Z₂. Based on the double beam Mach-Zehnder interference theory, the phase difference of the two interference modes and the central wavelength λ_m of m order interference fringe are respectively:

$$\varphi = \frac{2\pi(n_{eff}^{core1} - n_{eff}^{clad1})L_1}{\lambda} + \frac{2\pi(n_{eff}^{core2} - n_{eff}^{clad2})L_2}{\lambda} \quad (1)$$

$$\lambda_m = \frac{\Delta n_{eff1}L_1 + \Delta n_{eff2}L_2}{m} \quad (2)$$

Where n_{eff}^{core1} , n_{eff}^{clad1} and n_{eff}^{core2} , n_{eff}^{clad2} are 3PCF and 5PCF effective refractive indexes of fiber core mode and the corresponding cladding mode respectively, Δn_{eff1} and Δn_{eff2} are 3PCF and 5PCF effective refractive index difference between fiber core mode and cladding mode. λ is the free space optical wavelength, λ_m is the central wavelength of m order interference fringe, L_1 and L_2 are interference lengths, namely fused lengths of 3PCF and 5PCF.

The central wavelength of order interference fringe $m + 1$ is close to m order. By Eq. (2), it can be known that the central wavelength of $m + 1$ order interference fringe can be expressed as:

$$\lambda_{m+1} = \frac{\Delta n_{eff1}L_1 + \Delta n_{eff2}L_2}{m + 1} \quad (3)$$

By using Eqs. (2) and (3), it can be calculated the fringe interval between two contiguous wave peaks:

$$\Delta\lambda = \frac{\Delta n_{eff1}L_1 + \Delta n_{eff2}L_2}{m(m + 1)} \quad (4)$$

From Eqs. (2)–(4), it can be derived:

$$\Delta\lambda = \frac{\lambda_m \lambda_{m+1}}{\Delta n_{eff1}L_1 + \Delta n_{eff2}L_2} \quad (5)$$

In Eq. (5), for convenient calculation, also because there is a little difference between λ_m and λ_{m+1} , λ_m and λ_{m+1} , they could be regarded as equal to λ . Thus after being simplified, the fringes interval is:

$$\Delta\lambda = \frac{\lambda^2}{\Delta n_{eff1}L_1 + \Delta n_{eff2}L_2} \quad (6)$$

By Eq. (6), it can be seen that fringes interval is inversely proportional to effective refractive index difference and interference length, that is, the longer fused length is, the smaller fringes interval is.

Because of the effect of elastic-optic, when the bending curvature of the sensor changes, it makes the effective refractive index of fiber core mode and cladding mode change, then sensor transmission spectrum wavelength will drift. It can be known from Eq. (2), the wavelength drift caused by curvature change is

$$\begin{aligned} \Delta\lambda_m &= \left[\frac{(\Delta n_{eff1} + \Delta n_1)L_1}{m} - \frac{\Delta n_{eff1}L_1}{m} \right] + \left[\frac{(\Delta n_{eff2} + \Delta n_2)L_2}{m} - \frac{\Delta n_{eff2}L_2}{m} \right] \\ &= \frac{\Delta n_1 L_1}{m} + \frac{\Delta n_2 L_2}{m} \end{aligned} \quad (7)$$

where $\Delta\lambda_m$ is the center wavelength shift of m order interference fringe, Δn_1 and Δn_2 are the changes of 3 PCF and 5 PCF effective refractive indexes of fiber core mode and cladding mode, respectively. Thus different curvature can be measured by detecting the peak wavelength drift.

3. Experimental process and results analysis

3.1. Preparation of the sensors

Type SM-10 and SM-7 PCF solid core optical fiber used in the experiment are supplied by Yangze Optical Fiber & Cable Company. The cladding diameter is 125 μm . For SM-10 and SM-7 PCF solid core optical fiber, their core diameters are 9.5 μm and 7 μm , respectively. Each of them are made up of different layers of air holes, 3 and 5 layers, arranged in a hexagonal structure. And the air holes diameters are 5.46 μm and 2.82 μm separately, also distances between adjacent air holes are 3.35 μm and 5.43 μm respectively. Cross sections of SM-10 and SM-7 PCF are shown in Fig. 2.

FITEL-S178A type optical fiber fusion splicer is used for sensor preparation. In the experiment, the splice between PCF and SMF is carried out by manual splicing. During the splicing process, the splicing current is 30 mA, and discharge time is 750 ms. The wavelength range of ASE broadband light source is 1520–1610 nm, and the experimental data is recorded by AQ6375 Optical Spectrum Analyzer (OSA). Through repeated experiments, it can be confirmed that some of the air holes for both PCFs may be collapsed when the splicing length is set at 10 mm. Thus cladding modes can be stimulated better than other situations. Different fusion splicing joints are shown in Fig. 3.

In the experiments, at 30 mA for discharge current of optical fiber fusion splicer, the transmission spectra of cascading photonic crystal fiber sensor with splicing length at 10 mm, 15 mm, 20 mm respectively, are shown in Fig. 4.

Fig. 4 shows that as the sensors length increases, the interference fringe interval decreases. It exactly match with Eq. (6), showing that interference fringe interval has a close relationship with sensor length,

Download English Version:

<https://daneshyari.com/en/article/6888322>

Download Persian Version:

<https://daneshyari.com/article/6888322>

[Daneshyari.com](https://daneshyari.com)